Molecular Microbiology (2007) **66**(4), 1039–1050
doi:10.1111/j.1365-2958.2007.05975.x
First published online 23 October 2007

Novel mutations in ribosomal proteins L4 and L22 that confer erythromycin resistance in *Escherichia coli*

Sephorah Zaman, Megan Fitzpatrick, Lasse Lindahl and Janice Zengel*
Department of Biological Sciences, University of Maryland Baltimore County, 1000 Hilltop Circle, Baltimore, MD 21250, USA.

Summary

L4 and L22, proteins of the large ribosomal subunit, contain globular surface domains and elongated 'tentacles' that reach into the core of the large subunit to form part of the lining of the peptide exit tunnel. Mutations in the tentacles of L4 and L22 confer macrolide resistance in a variety of pathogenic and non-pathogenic bacteria. In *Escherichia coli*, a Lys-to-Glu mutation in L4 and a three-amino-acid deletion in the L22 had been reported. To learn more about the roles of the tentacles in ribosome assembly and function, we isolated additional erythromycin-resistant *E. coli* mutants. Eight new mutations mapped in L4, all within the tentacle. Two new mutations were identified in L22; one mapped outside the tentacle. Insertion mutations were found in both genes. All of the mutants grew slower than the parent, and they all showed reduced *in vivo* rates of peptide-chain elongation and increased levels of precursor 23S rRNA. Large insertions in L4 and L22 resulted in very slow growth and accumulation of abnormal ribosomal subunits. Our results highlight the important role of L4 and L22 in ribosome function and assembly, and indicate that a variety of changes in these proteins can mediate macrolide resistance.

Introduction

Many antibiotics, including members of the macrolide family, target the bacterial ribosome (Poehlsgaard and Douthwaite, 2005). Macrolide antibiotics bind to the bacterial large ribosomal subunit near the peptidyltransferase centre (PTC) at the beginning of the peptide exit tunnel (Schlunzen *et al*., 2001; Hansen *et al*., 2002a; Tu *et al*., 2005). Binding is thought to prevent progression of the growing peptide chain through the exit tunnel (Weisblum, 1995; Hansen *et al*., 2003; Tenson *et al*., 2003), leading to dissociation of the peptidyl tRNA from the ribosome (Menninger and Otto, 1982; Lovmar *et al*., 2004). Macrolide-resistant strains can arise via a number of different mechanisms, including methylation of A2058 in 23S rRNA by erm methyltransferases (Weisblum, 1995); mutation of 23S rRNA residues A2058, A2059 or A2062 (Vester and Douthwaite, 2001; Franceschi *et al*., 2004); and specialized efflux pumps (Poole, 2007).

Mutations in ribosomal proteins L4 and L22 can also cause macrolide resistance (Wittmann *et al*., 1973; Pardo and Rosset, 1977; Chittum and Champney, 1994; Franceschi *et al*., 2004). Like many other ribosomal proteins, L4 and L22 have globular domains on the surface of the ribosome and long tentacles that extend into the core of the ribosome. The tips of these extended loops form part of the lining of the exit tunnel (Ban *et al*., 2000; Nissen *et al*., 2000; Schuwirth *et al*., 2005), which is otherwise almost entirely lined by RNA (Ban *et al*., 2000). In bacterial species other than *Escherichia coli*, a variety of macrolide-resistant mutations in L4 and L22 have been identified (Franceschi *et al*., 2004), most of which map to the tentacles of L4 and L22. In *E. coli* only two erythromycin-resistant (ery-R) mutants have been characterized: strain N281 contains a deletion removing Met–Lys–Arg corresponding to codons 82–84 of L22, and strain N282 contains a change from lysine to glutamine at codon 63 of L4 (Apirion, 1967; Wittmann *et al*., 1973; Chittum and Champney, 1994).

Ribosomes from *E. coli* strain N282, containing the L4 mutation, bind erythromycin poorly, while ribosomes from N281, containing the mutant L22 protein, can still bind the antibiotic (Chittum and Champney, 1994). Furthermore, 50S subunit assembly is inhibited in the L22 mutant at high erythromycin concentrations, but assembly is unaffected in the L4 mutant (Chittum and Champney, 1995). The L4 mutant appears to reduce peptidyltransferase activity and increase levels of frameshifting, missense decoding, and readthrough of stop codons; peptidyltransferase activity and decoding are unaffected in the L22 mutant (Wittmann *et al*., 1973; O'Connor *et al*., 2004). Based on erythromycin binding and cryo-EM data of the two known *E. coli* mutants, it was proposed that the L4 mutation narrows the peptide exit tunnel so that

Accepted 25 September, 2007. *For correspondence. E-mail zengel@umbc.edu; Tel. 410-455-2876; Fax 410-455-3875.

Table 1. Properties of AB301 and ery-R derivatives.

Strain	# of isolates[a]	Doubling time (min)[b] –Ery	Doubling time (min)[b] +Ery	Max. ery resist. (mg ml^{-1})[c]	Max. spira resist. (mg ml^{-1})[d]	Max. tylosin resist. (mg ml^{-1})[e]	β-gal induction lag time (s)[f]	45S particles?[g] –Ery	45S particles?[g] +Ery	Fraction pre-23S[h]	Normalized ^{14}C-Ery = bound[i] –Ery	Normalized ^{14}C-Ery = bound[i] +Ery
AB301		30 (1.0)		< 0.1	< 1.0	1.0	130	–	–	0.03	1.00	0.47
L4-Q62K	1 (200)	57 (1.9)	83	1.5	3.0	> 6.0	160 (1.2)	–	–	0.12	0.03	0.04
L4-K63E (N282)	1 (150)	55 (1.8)	70	2.0	3.0	> 6.0	180 (1.4)	–	–		0.05	0.02
L4-G66S	1 (200)	36 (1.2)	70	0.5	1.5	2.0	140 (1.1)	–	–	0.08	0.56	0.19
L4-G66D	2 (150)	47 (1.6)	50	0.5	3.0	> 6.0	155 (1.2)	–	–	0.06	0.14	0.11
L4-G66R	1 (150)	65 (2.2)	78	1.0	3.0	> 6.0	160 (1.2)	–	–	0.11	0.01	0.04
L4-G66C	1 (200)	73 (2.4)	137	> 4.0	> 4.0	> 6.0	150 (1.2)	–	++	0.14	0.08	0.04
L4-56/6	1 (200)	103 (3.4)	115	2.0	3.0	> 6.0	200 (1.5)	+	+	0.16	0.01	0.01
L4-63/4	1 (150)	77 (2.6)	88	1.5	3.0	> 6.0	155 (1.2)	+	+	0.14	0.01	0.00
L4-72/6	1 (150)	121 (4.0)	122	> 4.0	> 4.0	> 6.0	200 (1.5)	+	+	0.17	0.00	0.01
L22-ΔMKR (N281)	0	50 (1.7)	50	1.5	1.5	4.0	150 (1.2)	–	–		0.74	0.42
L22-99/15	7 (150 and 200)	99 (3.3)	104	> 4.0	3.0	> 6.0	165 (1.3)	+++	+++	0.22	0.14	0.03
L22-105/2	1 (200)	59 (2.0)	57	2.5	3.0	> 6.0	150 (1.2)	±	++	0.12	0.68	0.19

a (column 1). In some cases we could not exclude that mutations found more than once arose from a single mutational event, so the numbers indicate the minimum number of isolates for each mutation. The values in parentheses indicate the concentration of erythromycin at which the mutant was isolated. L22-99/15 mutations were isolated at both 150 and 200 μg ml^{-1}; three isolates were analysed, two from 150 μg ml^{-1} erythromycin plates, and one isolated at 200 μg ml^{-1}. Their growth properties were indistinguishable.
b (column 2). Cells were grown at 37°C in LB. Values in parentheses indicate the growth rate normalized to the growth rate of AB301. Where indicated (+Ery), erythromycin was added to the concentration of the antibiotic used for the original isolation. Because AB301 does not grow at 150 or 200 μg ml^{-1} erythromycin, we studied its growth at 50 μg ml^{-1}, at which concentration it grew with a 95 min doubling time. Growth rates for each mutant were calculated for at least three cultures. For more complete data, including standard errors of the mean, see Fig. S1.
c–e (columns 3–5) Growth on LB plates containing various concentrations of antibiotics was scored as visible growth after 2 days at 37°C.
f (column 6). Values in parentheses indicate the lag time normalized to the AB301 value. For more details, see Fig. 2 and *Experimental procedures*.
g (column 7). The relative amounts of 45S particles are indicated as a range between no (–) and high (+++) amounts. Where indicated (+Ery), erythromycin was added to the concentration of the antibiotic used for the original isolation. The wild-type cells were grown at a sublethal (75 μg ml^{-1}) concentration of erythromycin. For more details, see Fig. 3.
h (column 8). The fraction of pre-23S rRNA was calculated as described in *Experimental procedures*.
i (column 9). The amount of ^{14}C-Ery (cpm) bound to ribosomes isolated from cells grown in the absence (–Ery) or presence (+Ery) was normalized to the amount bound to the wild-type parent ribosomes prepared from cells grown without erythromycin. The wild-type cells were grown at a sublethal (75 μg ml^{-1}) concentration of erythromycin. For more details, see Fig. S4.

erythromycin cannot enter to bind, while the L22 mutation widens the tunnel so that erythromycin binds but the nascent polypeptide is able to pass by (Gabashvili *et al*., 2001).

Given the variety of L4- and L22-mediated ery-R mutations observed in other species of bacteria (Franceschi *et al*., 2004), we reasoned that it should be possible to isolate additional mutations in the *E. coli* protein genes. If so, then such mutants could be used to further characterize the role of L4 and L22 (particularly, their tentacles) in ribosome assembly and function, as well as the mechanism(s) of macrolide resistance. Starting with *E. coli* strain AB301 (the parent of the two canonical ery-R mutant strains), we selected colonies that could grow on erythromycin. As predicted, we isolated novel mutations in these genes, including five missense and three insertion mutations in the L4 gene and two insertion mutations in the L22 gene. All but one mutation, a 6 bp insertion in L22, mapped within the tentacles of L4 and L22.

We have analysed the new *E. coli* L4 and L22 mutants, and observed effects on growth rate, peptide elongation rate and 23S rRNA processing. Some of the mutants also accumulated intermediate 45S particles. Our results not only provide insights into the mechanism of erythromycin resistance, but also highlight the important role of L4 and L22 in ribosome function and assembly.

Results

Identification of novel mutations in L4 and L22 genes

We selected spontaneous ery-R mutants from *E. coli* strain AB301 by spreading cells from overnight cultures on plates containing erythromycin at 150 or 200 μg ml^{-1}. About half of the colonies (33 out of 63) had a mutation in either L4 or L22. Because only two of the mutations were isolated more than once (Table 1, column 1), we have

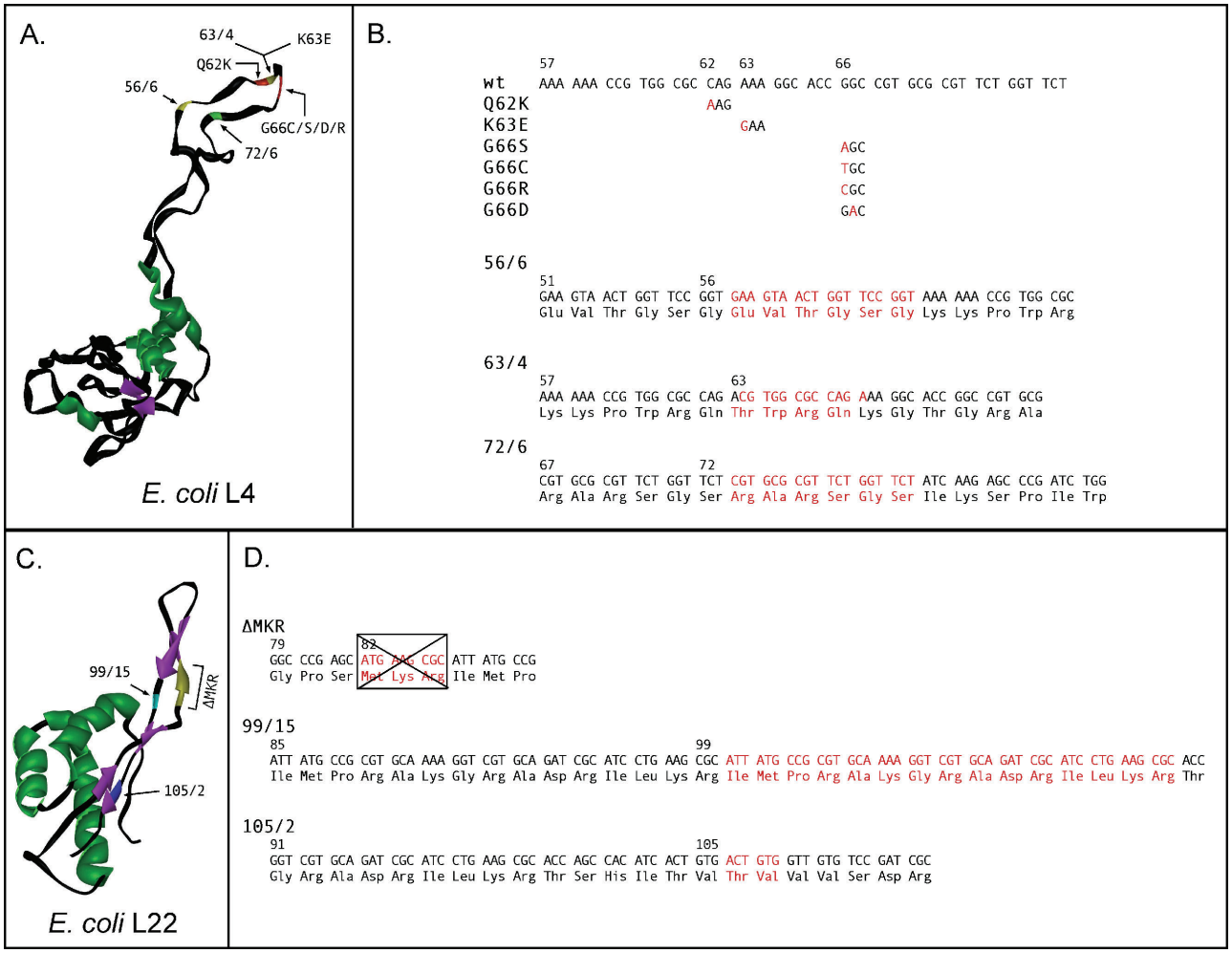

Fig. 1. Mutations in L4 and L22 conferring erythromycin resistance in *E. coli*.
A. Structure model of L4 (derived using CHIMERA from PDB file A2WB) showing locations of missense and insertion mutations in the tentacle of L4. Alpha helices are shown in green, and beta sheets are shown in purple.
B. Positions in the L4 gene of mutations conferring erythromycin resistance. Changes are indicated in red.
C. Structure model of L22 (derived using CHIMERA from PDB file A2WB) showing locations of deletion and insertion mutations in L22.
D. Positions in the L22 gene of mutations conferring erythromycin resistance. Changes are indicated in red.

almost certainly not saturated the two genes for erythromycin-resistance mutations.

In L4, all of the mutations mapped to the extended loop (Fig. 1A and B). Of the five new missense mutations, four were in the glycine codon at position 66 (L4-G66S, -G66C, -G66R, and -G66D) and one was in codon 62, causing a Gln-to-Lys change (L4-Q62K). In addition, we isolated the canonical mutation K63E (strain N282). Three large insertion mutations were also identified in L4. The insertions after codons 56 and 72 were 18 bp direct repeats of the DNA sequence immediately upstream (called L4-56/6 and L4-72/6, respectively), while the insertion within codon 63 was a 12 bp repeat (called L4-63/4).

Of the L22 mutations, one was in the extended loop (45 bp direct repeat insertion after codon 99, named L22-99/15), while one (6 bp direct repeat insertion after codon 105, called L22-105/2) was in the globular domain (Fig. 1C and D). We did not isolate the canonical ΔMKR mutant (strain N281). It is interesting that we isolated the L22-99/15 mutations seven times. Because cells carrying that mutation exhibited especially interesting properties (described below), we characterized three of the independent isolates; their phenotypes were indistinguishable (see, e.g. Fig. S1).

Growth of L4 and L22 mutants in the presence and absence of macrolides

The growth rates of the ery-R L4 and L22 mutants and the wild-type parent (AB301) were determined in LB liquid medium at 37°C with and without erythromycin (Table 1, column 2, and Fig. S1). In the absence of erythromycin,

the doubling time of the parent was approximately 30 min. All of the mutant strains grew more slowly, with doubling times up to four times the wild-type doubling time. Except for L22-105/2, the insertion mutant strains were especially slow. Addition of erythromycin further slowed the growth of all of the L4 missense mutant strains, as well as two of the L4 insertion mutants (Table 1, column 2, and Fig. S1). The L22 insertion mutants and L4-72/6 grew about as well when erythromycin was included in the media. None of the mutants exhibited significant temperature sensitivity (data not shown).

Although selected at 150 or 200 μg ml^{-1} erythromycin, the mutant strains were resistant on LB plates to at least 500 μg ml^{-1} erythromycin; several were resistant to 4 mg ml^{-1} erythromycin (Table 1, column 3). However, as expected from the liquid growth analysis, most of the mutants grew more slowly at even the lowest tested concentration of the antibiotic (100 μg ml^{-1}). We also tested the mutants for cross-resistance to other macrolide antibiotics, including spiramycin, tylosin and troleandomycin. Not surprisingly, all of the mutant strains showed increased resistance to these other macrolides (Table 1, columns 4 and 5, and data not shown).

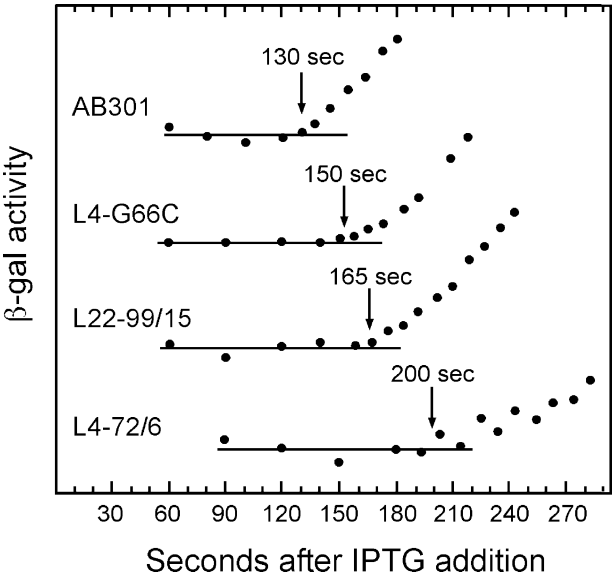

Fig. 2. β-Galactosidase induction lag times. Cells growing in minimal medium were induced with IPTG. Aliquots were removed and assayed at various times after induction (see *Experimental procedures*) to detect the time at which the enzyme activity increased above the basal level. Results for the wild-type parent and several of the mutants are shown. The *y*-axis represents arbitrary β-galactosidase activities, but the *x*-axis is the same for all the strains.

Reversion of L4 and L22 large insertion mutants grown in the absence of erythromycin

We observed that the insertion mutants (except for L22-105/2) grew much better after they had been grown overnight in antibiotic-free liquid media. Furthermore, when we streaked these mutant strains on LB and LB + erythromycin plates, we observed heterogeneous colony sizes on antibiotic-free plates (Fig. S2). To learn the cause of the faster-growing cells, we amplified and then sequenced the L4 and L22 genes from large and small colonies from each mutant. We found that the large colonies had reverted to the wild-type L4 and L22 sequences and regained sensitivity to erythromycin, while small colonies had retained the original insertions and erythromycin resistance. Thus, it appears that the large insertions were frequently removed from the L4 or L22 by a secondary mutation event that restored the wild-type sequence and growth rate.

Rate of translation elongation in L4 and L22 mutant strains

The reduced growth rates of the mutants suggest that ribosome function and/or assembly might be affected by mutations in L4 and L22. To investigate the effect on ribosome function, we measured the *in vivo* rate of peptide-chain elongation by measuring the time between isopropylthio-D-galactoside (IPTG) induction of transcription of the *lacZ* gene and the appearance of β-galactosidase activity above the basal level (Coffman *et al*., 1971). The parent strain had an induction lag of about 130 s (Table 1, column 6, and Fig. 2), corresponding to an elongation rate of 7.9 amino acids per second. Mutant strains had a lag that ranged from 140 s (7.3 aa s^{-1}) to 200 s (~5.1 aa s^{-1}) (Table 1, Fig. 2, and data not shown). Thus, the ery-R strains exhibited a decreased rate of chain elongation that roughly correlated with the growth defect. However, the difference is not sufficient to account for the substantially decreased growth rates of some of the mutants. For example, the L4 and L22 large insertion mutant strains have growth rates up to three times as long as that of wild type, but a β-galactosidase synthesis time that was less than twice that of the wild-type strain. It is important to note that this assay reflects the fastest rate of peptide elongation in the cell. If a heterogeneous population of ribosomes were present, the measured rate of elongation would reflect only the rate of the 'fastest' ribosomes, which might in principle be in the minority.

Ribosomal subunit assembly defects in L4 and L22 large insertion mutants

To determine whether the slow-growth phenotype could also be a result of defective ribosome assembly, we analysed ribosomal particles of wild-type and mutant strains using sucrose gradient analysis. Crude ribosomes from

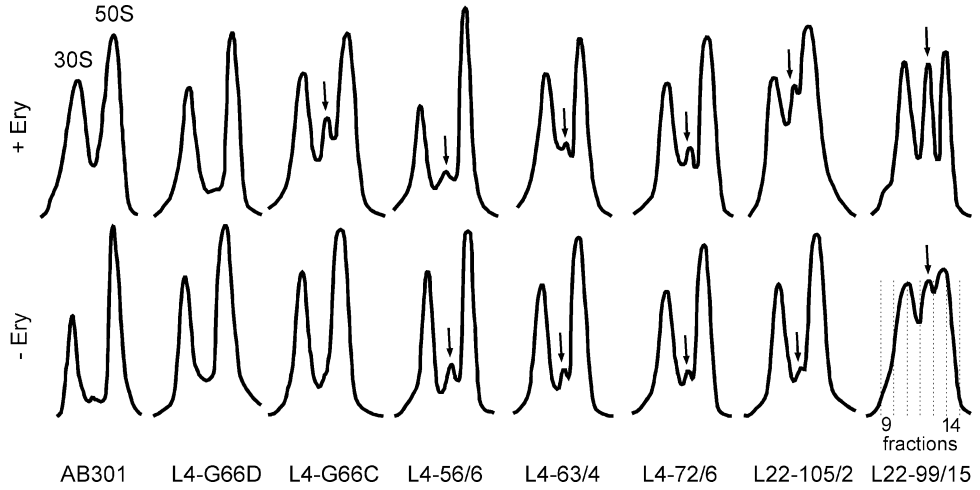

Fig. 3. Sucrose gradient sedimentation profiles of AB301 and ery-R mutants. Crude ribosomes isolated from cells grown in LB with (+Ery) or without (–Ery) erythromycin were centrifuged through a 10–50% (w/v) sucrose gradient prepared in buffer containing 1 mM $MgCl_2$ and 200 mM NH_4Cl. Absorption profiles were recorded at 260 nm. The absorption peaks of free 30S and 50S subunits are identified; aberrant ribosomal particles are indicated by vertical arrows. Fractions from the L22-99/15 –Ery gradient used later for primer extension (Fig. 4B) are indicated. The results for all of the mutants are summarized in Table 1, column 7.

wild-type and mutant strains were sedimented through sucrose gradients under conditions favouring dissociation of ribosomal subunits (1 mM $MgCl_2$, 200 mM NH_4Cl). In our initial experiments, we grew all of the ery-R mutants in the presence of erythromycin to avoid accumulation of revertants (described above). Under these growth conditions, most of the L4 missense mutants had a profile that was very similar to the pattern for the parent strain grown in the absence of erythromycin (Fig. 3, top, and data not shown). However, one of the L4 missense mutants (G66C), and all of the L4 and L22 insertion mutants, had abnormal profiles, with a new peak evident between the 30S and 50S peaks (Fig. 3, top). This peak, which we call 45S, was especially prominent in the L22 large insertion strains.

Because erythromycin has been shown to affect 50S subunit assembly (Chittum and Champney, 1995; Usary and Champney, 2001; Champney, 2006), we wanted to determine whether the aberrant profile was due to the presence of the antibiotic or the mutations in L4 and L22. The non-reverting L4-G66C strain and the stable L22-105/2 insertion mutant were grown in LB without erythromycin. The reverting strains were grown using an 'erythromycin chase' protocol (see *Experimental procedures*) consisting of initial growth in the presence of erythromycin and removal of the antibiotic, followed by growth without erythromycin for 2–4 doublings. Under these growth conditions, the 45S peak was diminished in L22-105/2 and disappeared from L4–66C profiles (Fig. 3, bottom), suggesting that for these mutants, the antibiotic was responsible for the aberrant peak. Interestingly, we did not observe this peak with ribosomes from AB301 grown in the presence of erythromycin: as reported previously (Usary and Champney, 2001), these wild-type ribosomes showed a decrease in the amount of 50S compared with 30S, but no evidence of an extra '45S' peak (Fig. 3).

The small aberrant peak observed with the L4 insertion mutants L4-56/6, L4-63/4 and L4-72/6 was present at about the same level with or without erythromycin (Fig. 3). Moreover, the large aberrant peak was still observed when the L22 large insertion mutant (L22-99/15) was grown in the absence of erythromycin (Fig. 3). The results of the sucrose gradient analysis are summarized in Table 1 (column 7). The accumulation of incomplete 45S particles correlates with the slow-growth phenotype of the large insertion mutants, and indicates that ribosome biogenesis is severely inhibited by the presence of large insertions in L4 and L22 independently of the erythromycin effect on assembly.

Processing of pre-23S rRNA in Ery-R mutant strains

Given that many of the mutants accumulated abnormal version(s) of the large ribosomal subunit, we investigated whether 23S rRNA processing was affected. Precursor 23S (pre-23S) rRNA generated by RNase III cleavage of the primary transcript is 7 nucleotides longer at the 5′ end than mature 23S RNA (King *et al*., 1984). We used primer extension analysis to determine the relative amounts of mature and pre-23S in wild-type and mutant strains. Total RNA extracted from cultures growing in mid-log phase was used as template, and an oligonucleotide complementary to the region ~75 nucleotides from the 5′ end of

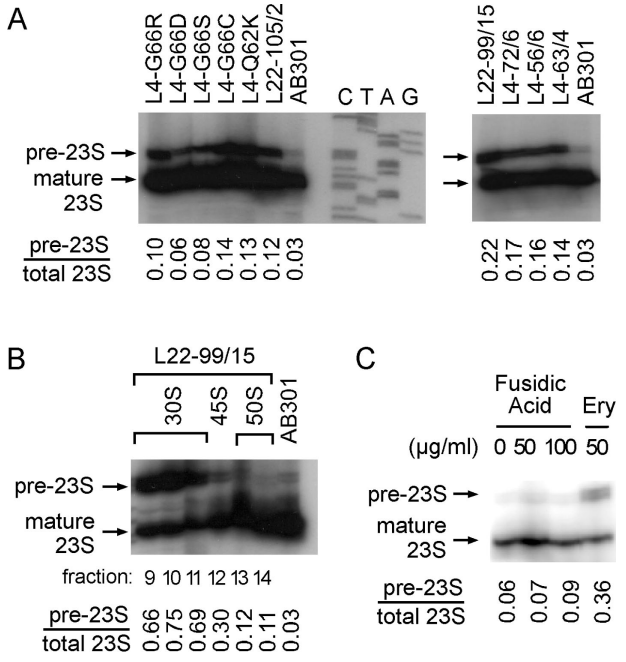

Fig. 4. Primer extension analysis of 23S rRNA in ery-R mutants.
A. Total RNA was purified from a mid-log phase culture and used as template. A ^{32}P-labelled oligonucleotide hybridizing internal to the 5′ end of 23S rRNA was used as the primer for the extension reaction. The products were analysed on a 8% acrylamide gel together with a sequencing ladder. Precursor and mature 23S rRNA are indicated.
B. RNA was extracted from L22-99/15 high-salt sucrose gradient fractions (see Fig. 3) and analysed by primer extension as described above. The AB301 lane contained RNA from a total-cell extract.
C. RNA was extracted from cells grown in LB containing the indicated concentration of fusidic acid or erythromycin, and analysed as described above.

23S RNA was used as primer. Two bands were detected in all the strains, corresponding in size to mature and pre-23S RNA (Fig. 4A). The fraction of pre-23S in the wild-type strain was 0.03. All of the mutant strains showed increased levels of the precursor form of 23S. The missense and short insertion mutant strains showed two- to almost fivefold increases, while the large insertion mutants showed a more dramatic increase, ranging from five- to sevenfold (Fig. 4A and Table 1, column 8). These results indicate that all of the L4 and L22 mutations correlate with a slower rate of rRNA processing.

The L22-99/15 mutant showed the highest level of pre-23S rRNA (22%), so we analysed it in more detail. To determine which ribosomal particles contain pre-23S, we extracted RNA from the fractions of the high-salt and low-Mg gradient of L22-99/15 ribosomes prepared from cells grown in the absence of erythromycin (Fig. 3, bottom right) and performed primer extension. We expected to find the pre-rRNA in the 45S particles, but found instead that the RNA colocalized with the 30S region of the gradient (Fig. 4B). These results reveal yet another class of precursor 50S particles, sedimenting with the 30S subunits.

We were concerned that the 23S processing defects were a result of, not a contributor to, the reduced growth rates in the mutant strains. To test the cause–effect relationship between growth rate and rRNA processing, we analysed the accumulation of pre-23S rRNA in wild-type cells grown in the presence of fusidic acid. This antibiotic interacts with the EF-G:ribosome complex to prevent release of EF-G–GDP, thereby inhibiting protein synthesis. At intermediate levels, the antibiotic decreases the rate of peptide-chain elongation, resulting in slower growth (Bennett and Maaløe, 1974). Unlike erythromycin, fusidic acid does not bind to the ribosome, and therefore, it should have no direct effect on ribosome biogenesis. Fusidic acid at 50 μg ml^{-1} changed the doubling time of AB301 from 28 to about 50 min, while at 100 μg ml^{-1}, the doubling time was further reduced to 70 min. For comparison, we also tested the effect of erythromycin, known to interfere with ribosome biogenesis (Champney, 2006). An erythromycin concentration of 50 μg ml^{-1} resulted in a doubling time of about 95 min. We then extracted total RNA from these cultures as well as the untreated cells, and analysed the 23S content by primer extension as explained above. We detected no significant effect on processing of 23S rRNA in the fusidic acid-treated cells (Fig. 4C). Therefore, we conclude that the accumulation of pre-23S rRNA in the ery-R mutant strains is not caused by the reduced growth rate, but is a direct result of the mutations' effect on ribosome assembly. Interestingly, erythromycin increased the pre-23S content about fivefold (Fig. 4C), indicating that the antibiotic's effect on ribosome assembly (Champney, 2006) includes an inhibition of 23S rRNA processing. A similar effect of erythromycin on processing of 23S rRNA has been seen by S. Champney (pers. comm.).

Incorporation of mutant L4 proteins into ribosomes

To confirm that the mutant L4 proteins from the ery-R mutant strains are incorporated into ribosomes, the presence of L4 was analysed by Western analysis of crude ribosomal pellets. We found that L4 was associated with crude ribosomes prepared from all of the mutant strains grown in the presence or in the absence of erythromycin (Fig. S3). In other studies, we have observed that certain mutant L4 proteins (not Ery-R mutations) are present in crude ribosomes but removed during a high-salt wash (our unpublished experiments). We reasoned that, among the L4 mutants, the insertions were most likely to result in an unstable association with 50S particles. Therefore, crude ribosomes from the L4 insertion mutant strains were salt-washed using 1 M NH_4Cl buffer and analysed by

Western analysis. We observed that salt-washing did not affect the association of the mutant proteins with the ribosome (data not shown).

We were not able to analyse the L22 mutant strains because we do not have an antibody that specifically recognizes this protein.

Erythromycin binding to mutant ribosomes

Erythromycin binds to the 50S subunit in a 1:1 stoichiometry in wild-type cells (Pestka, 1974). It has been shown previously that ery-R ribosomes with a three-amino-acid deletion in L22 (ΔMKR, strain N281) bind erythromycin with high affinity, while ery-R ribosomes with a Lys-to-Glu change at codon 63 in L4 (K63E, strain N282) show a much reduced affinity (Wittmann *et al*., 1973; Chittum and Champney, 1994). To learn more about the structures of the mutant ribosomes, we measured their ability to bind ^{14}C-labelled erythromycin using a nitrocellulose filter binding assay. As expected, the canonical L4-K63E ribosomes (strain N282) bound erythromycin very poorly (5% of parent AB301). Ribosomes from most of the other L4 mutants also showed little or no binding (Table 1, column 9). One surprising result was the almost normal binding of erythromycin to ribosomes from the G66S missense mutant (56%) ('-Ery' in Table 1, column 9).

Among the L22 mutants, ribosomes from the canonical ΔMKR mutant (strain N281) bound erythromycin nearly as well as AB301 (74% of wild type). Ribosomes from the L22-105/2 insertion mutant also bound erythromycin well (68%). However ribosomes from the L22-99/15 insertion mutant showed reduced binding (14% of wild type) (Table 1, column 9). Together, these binding studies indicate that not all L4 mutants fail to bind erythromycin, and not all L22 mutants bind the antibiotic well (see also Fig. S4).

Interestingly, ribosomes which showed significant binding to erythromycin (L4-G66S, L22-ΔMKR, and L22-105/2 and the wild-type parent AB301) also showed reduced binding when the ribosomes were prepared from cells grown in the presence of the antibiotic ('+Ery' in Table 1, column 9; see also Fig. S4). This reduction might result from an alteration in the structure of ribosomes assembled in the presence of erythromycin that occludes or distorts the antibiotic's target. Alternatively, unlabelled erythromycin bound to ribosomes during cell growth might remain bound to the ribosomes even through a high-salt centrifugation.

Discussion

We have identified new mutations in ribosomal proteins L4 and L22 that confer erythromycin resistance in *E. coli*. All mutations are located in the extended loop of L4 or L22, except for a short insertion mutation in the globular domain of L22. Mutations in r-protein L4 were especially easy to isolate; for example, a variety of amino acid substitutions near the tip of the tentacle confer erythromycin resistance. On the other hand, the variety of L22 mutations was much more limited, and included only two insertions. Although we have clearly not saturated the L4 and L22 genes for ery-R mutations, these results are consistent with our studies of ery-R mutants in the bacterium *Deinococcus radiodurans*: in this organism we were also able to isolate many more L4 mutants, including many missense mutations, than L22 mutants, which involved a deletion or an insertion (J. Zengel and L. Lindahl, manuscript in preparation). A variety of L4 and L22 tentacle mutations have also been identified in clinically relevant species of bacteria, including *Haemophilus influenzae*, *Streptococcus pyogenes* and *S. pneumoniae* (Franceschi *et al*., 2004). Many of these mutations, particularly for L22, also involve insertions and deletions.

We observed that the large insertion mutations in L4 and L22 tended to revert to wild-type in the absence of antibiotic. This phenomenon represents an interesting paradigm for antibiotic resistance, in which cells acquire mutations that help them survive in antibiotic medium but then avoid the high fitness cost of maintaining resistance mutations (evident from slower growth rates) by excising the insertion in an antibiotic-free environment. All insertions consist of direct repeats of the DNA sequence, which are removed precisely, presumably by recombination or 'slippage' during DNA replication or repair (Farabaugh *et al*., 1978; Albertini *et al*., 1982). On the other hand, no obvious repeats flank the insertion sites, so it is more difficult to speculate about the mechanism(s) creating the insertions. However, large insertion mutants could also be isolated in a *recA* mutant strain (our unpublished results), suggesting that the insertions are formed by 'slippage' during DNA replication or repair rather than by homologous recombination. Reversion is not observed in minimal media (our unpublished results), so slow-growth conditions might inhibit this process, possibly because of the lower number of genomes per cell at slow growth.

The large insertion mutant strains showed accumulation of 45S particles and of pre-23S rRNA containing a seven-nucleotide extension at the 5′ end. However, in mutant L22-99/15, most of this pre-23S rRNA was found in particles sedimenting at approximately 30S. Thus, it appears that the large insertions affect at least two steps of ribosome maturation. The failure to process pre-23S rRNA normally may be the result of the mutated proteins failing to shape an rRNA conformation that favours removal of the 5′ extension. We do not know whether the '30S' and 45S particles represent assembly intermediates or, instead, 'dead-end products' that contain improperly folded rRNA and/or that lack certain ribosomal proteins whose incorporation is stimulated by L4 or L22 in the

normal ribosomal assembly pathway(s). Precursor '30S' and 45S ribosomal particles have been reported previously in wild-type cells by pulse-labelling (Britten *et al*., 1962) and in various mutants (Guthrie *et al*., 1969; Tai *et al*., 1969); '30S' particles have also been observed in wild-type cells grown in sublethal concentrations of erythromycin (Usary and Champney, 2001). More recent experiments have shown that similar particles accumulate in *dnaK* mutant cells (El Hage and Alix, 2004); those particles could be chased into mature 50S (El Hage and Alix, 2004), suggesting that at least some of the various types of particles accumulating in mutant strains are genuine precursors. On the other hand, in both the L22-99/15 mutant and the *dnaK* mutant, the bulk of the pre-23S rRNA is found in the 30S region of sucrose gradients, while in exponentially growing wild-type *E. coli*, most of pre-23S rRNA is contained in 45–50S particles (Lindahl, 1975). Perhaps there are multiple pathways for ribosome assembly and maturation. Another possibility is that the kinetics of certain events, such as the conversion of pre-23S rRNA to mature 23S rRNA, are not strictly linked to steps in the construction of ribosomal particles.

In addition to the effect on rRNA processing and ribosome assembly, the ribosome translation rate is also reduced in the ery-R mutants. This observation suggests that changes in the tunnel resulting from mutations in L4 or L22 can be transmitted to the PTC region to affect the rate of peptide elongation. Our assay, measuring the time after induction at which β-galactosidase activity increases, can only reveal the elongation rate exhibited by the fastest ribosomes in the cell. If an L4 or L22 mutation results in a heterogeneous population of ribosomes, a fraction of the ribosomes might translate more slowly than the rate determined.

Our erythromycin binding assays indicate that one of the L4 mutants (L4-66S) exhibits strong erythromycin binding (56% of the parent), while one of the L22 mutants (L22-99/15) does not (14% of the parent). Therefore, the model of a narrower tunnel in L4 mutants and a widened tunnel in L22 mutants (Gabashvili *et al*., 2001) is not supported by our data, at least not as a general model. If the tunnel width is indeed affected by the L4 and L22 proteins, the relationship is complex. A serine at position 66 of L4 behaves differently from aspartic acid, cysteine or arginine at the same position. Given that these substitutions are in a glycine, a flexible amino acid close to the turn in the L4 tentacle, these mutations could have differential effects on L4 structure. On the other hand, all substitutions in position 66 result in similar levels of erythromycin resistance, suggesting that drug resistance can have several different molecular explanations.

Comparison of the sucrose gradients for L4-G66C and L22-99/15 cells grown with and without erythromycin (Fig. 3) indicates a significant effect of erythromycin on ribosomal assembly. This is unexpected, because ribosomes from these mutants have a poor affinity for the antibiotic. Perhaps the erythromycin binding site is accessible during ribosome assembly, but after assembly is completed, these mutations cause the site to be occluded so that binding is not detected in the *in vitro* assays. Alternatively, as suggested by Champney and coworkers (Champney and Burdine, 1995; Usary and Champney, 2001), the binding site for erythromycin during assembly may be different from the site in mature ribosomes. If this is the case, then our results suggest that the former site is less affected by mutations in L4 and L22. In any case, there is no evidence that erythromycin interacts directly with either protein (Schlunzen *et al*., 2001), so all of the mutations presumably have an indirect effect.

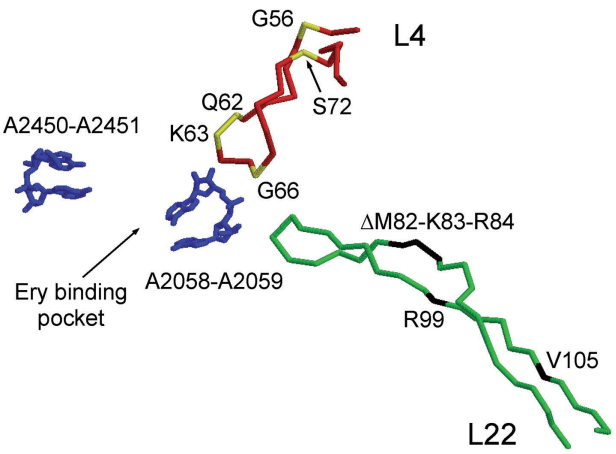

Fig. 5. Model of the L4 and L22 tentacles and key nucleotides in the PTC and PTC-proximal region of the tunnel. The backbones of the L4 (red) and L22 (green) tentacles are shown. Positions of point mutations, insertions and deletions are indicated in yellow for L4 and black for L22. Nucleotides are shown in blue. A2058 and A2059 are located the beginning of the tunnel and form part of the binding site for erythromycin and other macrolides. A2450 and A2451 are key nucleotides in the PTC (Nissen *et al*., 2000; Hansen *et al*., 2002b). The model was drafted using RasMol and PDB structure 2I2T (Berk *et al*., 2006).

The positions of the insertions into the L4 and L22 tentacles are as much as 40–70 Å from both the erythromycin binding site and the PTC (Fig. 5). A secondary cascade of modulations in the ribosome structure must therefore cause their effect on peptide growth rate and antibiotic binding. Direct evidence for structural modulations has been observed by cryo-electron microscopy of ribosomes from the original L4-K63E and L22-ΔMKR mutants (Gabashvili *et al*., 2001), as well as during stalling of the SecM peptide in wild-type cells in the ribosome exit tunnel (Mitra *et al*., 2006). Chemical probing experiments by Gregory and Dahlberg (1999) also identified perturbations in the rRNA structures in L4-K63E and L22-ΔMKR ribosomes. Therefore, it is not surprising that similar effects might emanate from our new mutations in

L4 and L22, particularly in the case of the largest insertions. For example, L22 is a small, 110-amino-acid protein, so a 45 bp insertion mutation signifies a significant increase in its size. The variations in the ribosome properties observed in our mutants suggest that these cascades of structural modifications can play out in different ways. Chemical probing or other structure analysis will be required to determine how this extra bulk in the L22 and L4 proteins affects the rRNA structure.

Experimental procedures

Isolation of ery-R mutants

The wild-type strain used in this study is *E. coli* strain AB301 (A19 Hfr met$^-$). Erythromycin-resistant strains N281 and N282, carrying mutations in r-proteins L22 and L4 respectively, have been described previously (Wittmann *et al*., 1973; Chittum and Champney, 1994). The minimal inhibitory concentration of erythromycin for AB301 was determined to be 150 μg ml^{-1}. In the first selection, a single colony from strain AB301 was used to inoculate LB broth. After overnight growth at 37°C, 0.1 ml aliquots was plated on LB agar + 150 or 200 μg ml^{-1} erythromycin (Sigma) and incubated at 37°C for up to 5 days. In a second selection, strain AB301 was plated on LB-agar plates without erythromycin. The single colonies obtained were grown in 0.3 ml LB broth (without erythromycin) in a 24-well plate (one colony per well). Approximately 0.1 ml from each well was plated on LB + 150 μg ml^{-1} erythromycin. If more than one mutant grew on a plate, only one was repurified. The latter selection protocol ensured that independent mutants were isolated.

Polymerase chain reaction (PCR) amplification and DNA sequencing

The L4 and L22 genes (*rplD* and *rplV*, respectively) from ery-R colonies were amplified by colony PCR using primers O1462 (5′-CTGGTTAAAGGTGCTGTCC-3′) and O1455 (5′-CCATCGCAGTAGACGCTT-3′) to amplify the L4 gene, and primers O1460 (5′-GAATTCGCACCGACTCGTAC-3′) and O1461 (5′-GGTGTTCGCAAAGGTGCTGTCCC-3′) to amplify the L22 gene. PCR products were purified using a Qiaquick PCR purification kit (Qiagen) and sequenced with the ABI Big Dye terminator sequencing kit using primers O1462 and O1460. To confirm that the identified changes in the L4 or L22 genes were responsible for the mutants' phenotypes, we amplified the relevant gene and, by recombineering, introduced the DNA into one or more other hosts. For all of the mutations, the resulting strains maintained the phenotypic properties of the original mutants (M. Lawrence and J.M. Zengel, data not shown).

Analysis of erythromycin, spiramycin and tylosin resistance

To determine the mutants' level of resistance to erythromycin, spiramycin and tylosin, AB301, N281, N282 and the new ery-R mutants were streaked onto LB-agar plates supplemented with various amounts of the antibiotics. Plates were incubated at 37°C for 2 days before growth was scored.

Growth rate assay and identification of revertants

Growth rates were measured for cells growing exponentially at 37°C. For growth rates measured in the presence of erythromycin, mutant strains were grown in LB containing erythromycin at the same concentration as that at which they were isolated (150 or 200 μg ml^{-1}). For growth rates measured in the absence of erythromycin, non-reverting strains (missense and short insert mutants) were grown in LB without erythromycin. Reverting strains were grown in LB + erythromycin. When the density reached OD_{450} = 1.0–1.2 (approximately 2×10^8 cells per ml), the culture was filtered through a 0.22 μm cellulose acetate filter (Corning). The trapped cells were washed twice with prewarmed LB without erythromycin, resuspended in sixfold the original culture volume LB without erythromycin (prewarmed), and incubated again at 37°C. Revertants were identified by streaking strains on LB and LB + erythromycin (150 or 200 μg ml^{-1}) plates. The L4 and L22 genes from single colonies were amplified by colony PCR and sequenced as described above.

Ribosome preparation

Non-reverting strains were grown at 37°C in LB with or without erythromycin. Reverting strains were grown with erythromycin or in a 'chase' experiment as described above. When the cultures reached OD_{450} = 1.5–2.0 (mid-log phase), cells were harvested by pouring onto ice and pelleting at 8K for 10 min. Cells were resuspended in buffer A (20 mM HEPES-KOH pH 7.5, 6 mM $MgCl_2$, 30 mM NH_4Cl, 6 mM β-mercaptoethanol) and lysed using the slow-thaw lysozyme method (Zengel *et al*., 2003). Cell debris was removed by spinning at 22K for 30 min, and the supernatant was used as the crude cell lysate. The cell lysate was spun at 50K for 4 h to pellet crude ribosomes. Ribosome pellets were washed with buffer A and resuspended overnight in 200 μl buffer A. To prepare salt-washed ribosomes, 100 μl of crude ribosomes was added to 0.9 ml salt wash buffer (20 mM HEPES-KOH pH 7.5, 30 mM $MgCl_2$, 1 M NH_4Cl, 6 mM β-mercaptoethanol), incubated for 1 h on ice, spun at 50K for 4 h, and resuspended as for crude ribosomes.

Erythromycin binding

Erythromycin binding assays were performed by the method of Teraoka (1970). Briefly, ribosomes (2.5 A_{260} units) were incubated at 37° for 15 min with 2–5 μl of a 1:100 dilution of [N-methyl-^{14}C]-erythromycin (New England Nuclear; 55 mCi-mmol^{-1}; 100 μCi ml^{-1}) in erythromycin binding buffer (50 mM Tris-HCl pH 7.8; 16 mM Mg acetate; 60 mM KCl; 100 μl final volume). Each reaction contained 36–90 pmol erythromycin and 50–60 pmole ribosomes [assuming 1 mg ml^{-1} *E. coli* ribosomes corresponds to 18 A_{260} (Haselkorn *et al*., 1963)]. The assay mix was poured through a 0.45 μm nitrocellulose filter (Millipore). Filters were washed three times, each with 2 ml erythromycin wash buffer (25 mM Tris-HCl pH 7.8, 20 mM

Mg acetate, 60 mM KCl). The amount of radioactive erythromycin bound to the ribosomes was measured by liquid scintillation counting of the filters (Beckman-Coulter LS 6500). Assays were always carried out in duplicate or triplicate.

Induction of β-galactosidase

The kinetics of induction of β- galactosidase were determined as described (Zengel *et al*., 1977). Briefly, cultures were grown at 30°C in AB minimal media (Clark and Maaløe, 1967) supplemented with glycerol (0.4%), thiamine (1 μg ml^{-1}) and casamino acids (0.1%). At OD_{450} between 0.2 and 0.45, the gratuitous inducer IPTG was added to a final concentration of 1 mM. Samples were removed at various times after addition of IPTG and mixed immediately with Z buffer (Miller, 1972) plus 50 μl 1% deoxycholate, 10 μl chloramphenicol (10 mg ml^{-1} in ethanol) and 40 μl toluene at 0°C (total volume 1 ml). After evaporation of toluene and ethanol, the β-galactosidase activity was measured as hydrolysis of o-nitrophenyl-β-D-galactoside according to the procedure of Miller (1972).

Sucrose gradient sedimentation

Crude ribosomes (10 A_{260} units) were incubated at 0°C for 45 min in 2× to 10× volume buffer A-3 (20 mM HEPES-KOH pH 7.5, 1 mM $MgCl_2$, 200 mM NH_4Cl, 6 mM β-mercaptoethanol), loaded on top of 10–50% sucrose gradients in buffer A-3, and centrifuged at 4°C for 16 h at 24 500 r.p.m. Fractions were collected using an ISCO sucrose gradient collector with a UV monitor.

Primer extension

Total RNA was isolated by the hot phenol method from cultures grown to mid-log phase (Zengel *et al*., 1990). Primers hybridizing ~75 nt internal to the 5′ end of mature 23S rRNA were end-labelled with [γ-^{32}P]-ATP by T4 kinase using standard protocols (Sambrook *et al*., 1989). Radiolabelled primer (10^6 cpm) was mixed with 5 μg ethanol-precipitated RNA in 0.5 M Tris-HCl pH 8/1 M KCl buffer, incubated at 90°C for 1 min, and slowly cooled to room temperature. The RNA–primer mixture was mixed with First Strand Buffer (Invitrogen), 6.5 mM dithiothreitol, 0.1 mM deoxyribonucleoside triphosphates, 10 U ribonuclease inhibitor (Fermentas) and 200 U Superscript III Reverse Transcriptase (Invitrogen), and incubated at room temperature for 5 min and then at 50°C for 45 min. Reactions were terminated by the addition of 2 μl 0.25 M EDTA, extracted using 1:1 phenol/chloroform/isoamylalcohol, followed by chloroform extraction, ethanol precipitated, and resuspended in 4 μl H_2O. RNA loading buffer (4 μl) was added and the sample was heated at 70°C for 4 min. A 4 μl aliquot was analysed by electrophoresis on an 8% sequencing gel. For size markers, a sequencing ladder was run alongside the samples. To quantify the radioactivity in bands representing mature and pre-23S rRNAs, the gel was dried using a vacuum blotter at 76°C for 2 h and analysed on a phosphorimager (Molecular Dynamics).

RNA was extracted from 0.5 ml sucrose gradient fractions by phenol extraction and ethanol precipitation, and analysed by primer extension as described above.

Western analysis

Crude and salt-washed ribosomes (0.33 A_{260} units) were fractionated by 12% SDS-PAGE (Laemmli, 1970) and subjected to Western analysis as described (Zengel *et al*., 2003). Prestained molecular weight markers (Fermentas PAGE Ruler) were used. For probing L4, a rabbit polyclonal antibody specific for *E. coli* L4 (a gift from M. Nomura, diluted 1:10 000) was used as the primary antibody. An alkaline phosphatase-conjugated goat-anti rabbit IgG (Bio-Rad, diluted 1:3000) was used as the secondary antibody. The signal was detected by chemiluminescence using the CDP-STAR substrate (Sigma-Aldrich).

Acknowledgements

This work was supported by Grant MCB 03499443 from the National Science Foundation. We thank Susan Fretz for excellent technical assistance, and members of our laboratory for valuable discussions.

References

Albertini, A.M., Hofer, M., Calos, M.P., and Miller, J.H. (1982) On the formation of spontaneous deletions: the importance of short sequence homologies in the generation of large deletions. *Cell* **29:** 319–328.

Apirion, D. (1967) Three genes that affect *Escherichia coli* ribosomes. *J Mol Biol* **30:** 255–275.

Ban, N., Nissen, P., Hansen, J., Moore, P.B., and Steitz, T.A. (2000) The complete atomic structure of the large ribosomal subunit at 2.4 Å resolution. *Science* **289:** 905–920.

Bennett, P.M., and Maaløe, O. (1974) The effects of fusidic acid on growth, ribosome synthesis and RNA metabolism in *Escherichia coli*. *J Mol Biol* **90:** 541–561.

Berk, V., Zhang, W., Pai, R.D., and Cate, J.H. (2006) Structural basis for mRNA and tRNA positioning on the ribosome. *Proc Natl Acad Sci USA* **103:** 15830–15834.

Britten, R.J., McCarthy, B., and Roberts, R.B. (1962) The synthesis of ribosomes in *E. coli*. IV. The synthesis of ribosomal protein and the assembly of ribosomes. *Biophys J* **2:** 83–93.

Champney, W.S. (2006) The other target for ribosomal antibiotics: inhibition of bacterial ribosomal subunit formation. *Infect Disord Drug Targets* **6:** 377–390.

Champney, W.S., and Burdine, R. (1995) Macrolide antibiotics inhibit 50S ribosomal subunit assembly in *Bacillus subtilis* and *Staphylococcus aureus*. *Antimicrob Agents Chemother* **39:** 2141–2144.

Chittum, H.S., and Champney, W.S. (1994) Ribosomal protein gene sequence changes in erythromycin-resistant mutants of *Escherichia coli*. *J Bacteriol* **176:** 6192–6198.

Chittum, H.S., and Champney, W.S. (1995) Erythromycin inhibits the assembly of the large ribosomal subunit in growing *Escherichia coli* cells. *Curr Microbiol* **30:** 273–279.

Clark, D.J., and Maaløe, O. (1967) DNA replication and the division cycle in *Escherichia coli*. *J Mol Biol* **23:** 99–112.

Coffman, R.L., Norris, T.E., and Koch, A.L. (1971) Chain elongation rate of messenger and polypeptides in slowly growing *Escherichia coli*. *J Mol Biol* **60:** 1–19.

El Hage, A., and Alix, J.H. (2004) Authentic precursors to ribosomal subunits accumulate in *Escherichia coli* in the absence of functional DnaK chaperone. *Mol Microbiol* **51:** 189–201.

Farabaugh, P.J., Schmeissner, U., Hofer, M., and Miller, J.H. (1978) Genetic studies of the *lac* repressor. VII. On the molecular nature of spontaneous hotspots in the *lacI* gene of *Escherichia coli*. *J Mol Biol* **126:** 847–857.

Franceschi, F., Kanyo, Z., Sherer, E.C., and Sutcliffe, J. (2004) Macrolide resistance from the ribosome perspective. *Curr Drug Targets Infect Disord* **4:** 177–191.

Gabashvili, I.S., Gregory, S.T., Valle, M., Grassucci, R., Worbs, M., Wahl, M.C., *et al.* (2001) The polypeptide tunnel system in the ribosome and its gating in erythromycin resistance mutants of L4 and L22. *Mol Cell* **8:** 181–188.

Gregory, S.T., and Dahlberg, A.E. (1999) Erythromycin resistance mutations in ribosomal proteins L22 and L4 perturb the higher order structure of 23 S ribosomal RNA. *J Mol Biol* **289:** 827–834.

Guthrie, C., Nashimoto, H., and Nomura, M. (1969) Structure and function of *E. coli* ribosomes. 8. Cold-sensitive mutants defective in ribosome assembly. *Proc Natl Acad Sci USA* **63:** 384–391.

Hansen, J.L., Ippolito, J.A., Ban, N., Nissen, P., Moore, P.B., and Steitz, T.A. (2002a) The structures of four macrolide antibiotics bound to the large ribosomal subunit. *Mol Cell* **10:** 117–128.

Hansen, J.L., Schmeing, T.M., Moore, P.B., and Steitz, T.A. (2002b) Structural insights into peptide bond formation. *Proc Natl Acad Sci USA* **99:** 11670–11675.

Hansen, J.L., Moore, P.B., and Steitz, T.A. (2003) Structures of five antibiotics bound at the peptidyl transferase center of the large ribosomal subunit. *J Mol Biol* **330:** 1061–1075.

Haselkorn, R., Fried, V.A., and Dahlberg, J.E. (1963) Cell-free protein synthesis: the association of viral RNA and *E. coli* ribosomes. *Proc Natl Acad Sci USA* **49:** 511–517.

King, T.C., Sirdeshmukh, R., and Schlessinger, D. (1984) RNase III cleavage is obligate for maturation but not for function of *Escherichia coli* pre-23S rRNA. *Proc Natl Acad Sci USA* **81:** 185–188.

Laemmli, U.K. (1970) Cleavage of structural proteins during the assembly of the head of bacteriophage T4. *Nature* **227:** 680–685.

Lindahl, L. (1975) Intermediates and time kinetics of the *in vivo* assembly of *Escherichia coli* ribosomes. *J Mol Biol* **92:** 15–37.

Lovmar, M., Tenson, T., and Ehrenberg, M. (2004) Kinetics of macrolide action: the josamycin and erythromycin cases. *J Biol Chem* **279:** 53506–53515.

Menninger, J.R., and Otto, D.P. (1982) Erythromycin, carbomycin, and spiramycin inhibit protein synthesis by stimulating the dissociation of peptidyl-tRNA from ribosomes. *Antimicrob Agents Chemother* **21:** 811–818.

Miller, J.H. (1972) *Experiments in Molecular Genetics*. Cold Spring Harbor, NY: Cold Spring Harbor Laboratory Press.

Mitra, K., Schaffitzel, C., Fabiola, F., Chapman, M.S., Ban, N., and Frank, J. (2006) Elongation arrest by SecM via a cascade of ribosomal RNA rearrangements. *Mol Cell* **22:** 533–543.

Nissen, P., Hansen, J., Ban, N., Moore, P.B., and Steitz, T.A. (2000) The structural basis of ribosome activity in peptide bond synthesis. *Science* **289:** 920–930.

O'Connor, M., Gregory, S.T., and Dahlberg, A.E. (2004) Multiple defects in translation associated with altered ribosomal protein L4. *Nucleic Acids Res* **32:** 5750–5756.

Pardo, D., and Rosset, R. (1977) Properties of ribosomes from erythromycin resistant mutants of *Escherichia coli*. *Mol Gen Genet* **156:** 267–271.

Pestka, S. (1974) Binding of [^{14}C]erythromycin to *Escherichia coli* ribosomes. *Antimicrob Agents Chemother* **6:** 474–478.

Poehlsgaard, J., and Douthwaite, S. (2005) The bacterial ribosome as a target for antibiotics. *Nat Rev Microbiol* **3:** 870–881.

Poole, K. (2007) Efflux pumps as antimicrobial resistance mechanisms. *Ann Med* **39:** 162–176.

Sambrook, J., Fritsch, E.F., and Maniatis, T. (1989) *Molecular Cloning.* Cold Spring Harbor, NY: Cold Spring Harbor Laboratory Press.

Schlunzen, F., Zarivach, R., Harms, J., Bashan, A., Tocilj, A., Albrecht, R., *et al.* (2001) Structural basis for the interaction of antibiotics with the peptidyl transferase centre in eubacteria. *Nature* **413:** 814–821.

Schuwirth, B.S., Borovinskaya, M.A., Hau, C.W., Zhang, W., Vila-Sanjurjo, A., Holton, J.M., and Cate, J.H. (2005) Structures of the bacterial ribosome at 3.5 Å resolution. *Science* **310:** 827–834.

Tai, P.C., Kessler, D.P., and Ingraham, J. (1969) Cold-sensitive mutations in *Salmonella typhimurium* which affect ribosome synthesis. *J Bacteriol* **97:** 1298–1304.

Tenson, T., Lovmar, M., and Ehrenberg, M. (2003) The mechanism of action of macrolides, lincosamides and streptogramin B reveals the nascent peptide exit path in the ribosome. *J Mol Biol* **330:** 1005–1014.

Teraoka, H. (1970) A reversible change in the ability of *Escherichia coli* ribosomes to bind to erythromycin. *J Mol Biol* **48:** 511–515.

Tu, D., Blaha, G., Moore, P.B., and Steitz, T.A. (2005) Structures of MLSBK antibiotics bound to mutated large ribosomal subunits provide a structural explanation for resistance. *Cell* **121:** 257–270.

Usary, J., and Champney, W.S. (2001) Erythromycin inhibition of 50S ribosomal subunit formation in *Escherichia coli* cells. *Mol Microbiol* **40:** 951–962.

Vester, B., and Douthwaite, S. (2001) Macrolide resistance conferred by base substitutions in 23S rRNA. *Antimicrob Agents Chemother* **45:** 1–12.

Weisblum, B. (1995) Erythromycin resistance by ribosome modification. *Antimicrob Agents Chemother* **39:** 577–585.

Wittmann, H.G., Stoffler, G., Apirion, D., Rosen, L., Tanaka, K., Tamaki, M., *et al.* (1973) Biochemical and genetic studies on two different types of erythromycin resistant mutants of *Escherichia coli* with altered ribosomal proteins. *Mol Gen Genet* **127:** 175–189.

Zengel, J.M., Young, R., Dennis, P.P., and Nomura, M. (1977) Role of ribosomal protein S12 in peptide chain

elongation: analysis of pleiotropic, streptomycin-resistant mutants of *Escherichia coli*. *J Bacteriol* **129:** 1320–1329.
Zengel, J.M., McCormick, J.R., Archer, R.H., and Lindahl, L. (1990) A hybrid selection technique for analysing *E. coli* mRNA: applications to the study of ribosomal protein operons. In *Ribosomes and Protein Synthesis: A Practical Approach*. Spedding, G. (ed.). New York, NY: Oxford University Press, pp. 213–227.
Zengel, J.M., Jerauld, A., Walker, A., Wahl, M.C., and Lindahl, L. (2003) The extended loops of ribosomal proteins L4 and L22 are not required for ribosome assembly or L4-mediated autogenous control. *RNA* **9:** 1188–1197.

Supplementary material

This material is available as part of the online article from:
http://www.blackwell-synergy.com/doi/abs/10.1111/j.1365-2958.2007.05975.x
(This link will take you to the article abstract).

Please note: Blackwell Publishing is not responsible for the content or functionality of any supplementary materials supplied by the authors. Any queries (other than missing material) should be directed to the corresponding author for the article.

